Enhanced Sensitivity of SAW-Based Pirani Vacuum Pressure Sensor

K. J. Singh, O. Elmazria, F. Sarry, P. Nicolay, K. Ghoumid, B. Belgacem, D. Mercier, J. Bounouar

Enhanced Sensitivity of SAW-Based Pirani Vacuum Pressure Sensor

Kanwar J. Singh, Omar Elmazria, Frederic Sarry, Pascal Nicolay, Kamal Ghoumid, Brahim Belgacem, Denis Mercier, and Julien Bounouar

***Abstract*—The authors have already presented a novel surface acoustic wave device for vacuum pressure measurement by employing a piezoelectric substrate that has a high value of temperature coefficient of frequency. Frequency-shift measurements as a function of vacuum pressure can be used to extract information about the pressure sensitivity of the device. In this paper, we report that the deposition of an aluminum thin-film layer and rise in the sensor's operating temperature significantly improve the sensitivity of the device. The results are crucial for improving the lower limit of the vacuum pressure measurement, which currently stands around 10^{-3} Pa.**

***Index Terms*—Acoustic devices, frequency response, pressure measurements, sensitivity.**

I. Introduction

A CONVENTIONAL Pirani gauge consists of a hot wire and temperature-dependent resistor in a vacuum tube. Higher pressure implies more gas molecules in contact with the wire which, in turn, increases heat conduction. This phenomenon leads to a reduction in temperature of the wire which causes a change in resistance values of the resistor. Vacuum pressure is measured in terms of varying resistance values. The conventional Pirani gauge is sensitive in the vacuum pressure region of 10^{-1} up to 100 Pa [1]. There have been several attempts in the recent years to improve the lower and higher vacuum pressure sensitivity limits of Pirani gauges, for example, by employing suspending structures, varying the gap between heater and sink etc. [2]–[6]. The principle of the presented sensor is similar to the Pirani sensor. Temperature variations due to pressure changes (or a change in the number of gas molecules) in the chamber are detected by the change in frequency values of surface acoustic wave (SAW) instead of a variation in resistance values as in the case of the conventional Pirani gauge and, hence, the sensor has been abbreviated as the Pirani SAW sensor [7], [8]. Our device uses the novel concept to measure subatmospheric pressure by taking advantage of high SAW thermal sensitivity as observed in many piezoelectric materials. It is possible to detect minute temperature variations in the medium by employing SAW substrates with high-temperature coefficient of frequency (TCF) values. When the substrate is heated with the constant power in the gas at given thermal and pressure conditions, its equilibrium temperature is determined by the heating power and energy loss. The energy loss is related to the thermal conductivity of gas (conduction), convection, and radiation heat loss. At low pressure (Knudsen regime), convection does not occur, radiation is independent of pressure, and conduction decreases with pressure. Therefore, after determining the temperature-pressure relationship, pressure values can be determined from the measured equilibrium temperatures. By using SAW devices, which employ substrates with high TCF values, it has become possible to probe temperature (in terms of SAW frequency) with high precision and, hence, discriminate small pressure steps [7].

The vacuum sensing range of the Pirani SAW sensor is much wider compared to the conventional Pirani sensor. The Pirani SAW sensor can sense the vacuum pressure in the pressure range of 10^{-3} up to 10^{5} Pa. Currently, our research area of interest is to extend the sensing limit of lower vacuum pressure down to 10^{-4} Pa. Due to a small number of air molecules below 10^{-3} Pa, the task is difficult. One of the possibilities to achieve this target is to increase the sensitivity of the SAW device. Although it has been speculated theoretically that the coating of low emissivity metal on the piezoelectric material can improve the sensitivity of SAW vacuum pressure sensor, it has not been yet confirmed experimentally [7], [8].

Several types of substrates are used during the fabrication of SAW devices [9]–[11]. Lithium niobate ($LiNbO_3$), langasite, lithium tantalate ($LiTaO_3$), and quartz are the most commonly used materials as substrates [12]. Depending upon the nature of the application of the device and its requirement, suitable substrates can be selected. Due to their low TCF or almost zero value at room temperature, quartz or langasite are the best materials when thermal stability is required. For example, they can be used in the technical areas, such as high stability resonators or narrowband filters. On the other hand, $LiNbO_3$ and $LiTaO_3$ are widely used in communication systems as wideband filters due to their high electromechanical coupling coefficient and TCF values [9], [11]. For the reported experiments,

K. J. Singh, on leave from the Physics Department, Guru Nanak Dev University, Amritsar, India, is with Institut Jean Lamour, Nancy 54506, France (e-mail: kanwarjitsingh@yahoo.com).

O. Elmazria and F. Sarry are with Institut Jean Lamour, Nancy 54506, France.

P. Nicolay is with EPCOS S.A.S., World Trade Center, Valbonne Sophia Antipolis 06560, France

K. Ghoumid is with FEMTO-ST, Besancon 25044, France.

B. Belgacem is with Senseor, Besançon 25000, France.

D. Mercier is with CEA-LETI-MINATEC, Grenoble 38054, France.

J. Bounouar is with ADIXEN, ALCATEL Vacuum Technology France (AVTF), Annecy 74009, France.

we have chosen $LiNbO_3$ due to its high value of TCF. Several studies have reported the normal (conventional or white) $LiNbO_3$ but few data are presented for black $LiNbO_3$. Chemically reduced $LiNbO_3$, popularly known as black $LiNbO_3$ due to its gray to dark black color, has many advantages over the conventional $LiNbO_3$. Some of them are as follows [13], [14]: 1) due to a higher value of optical absorption, photolithographic processing becomes easier and precise and 2) pyroelectric sparking can be effectively decreased due to higher values of electrical conductivity. Pyroelectric sparking can lead to electrical surface charging, device performance failure, and catastrophic crystal fracture. Therefore, it is estimated that in the near future, black $LiNbO_3$ may be a preferable substrate over conventional $LiNbO_3$ for the development of several commercial products.

Continuous improvements in photolithography techniques have resulted in the development of several cheap, miniature, and highly functional microelectromechanical-systems (MEMS) devices. MEMS and interdigital-transducer (IDT) technology-based SAW devices have advantages in terms of cost and small size. Moreover, they can be requested remotely and, hence, they can be used under harsh environments, such as high temperatures, nuclear reactors, etc.

In light of the aforementioned situation, the authors have undertaken the study of the effect of the deposition of thin-film low emissivity metal (aluminum in our case) at the backside of the black $LiNbO_3$ substrate on the pressure sensitivity of the acoustic device. The Pirani SAW device employs MEMS-IDT technology.

II. Theory

The theoretical evaluation of sensitivity as a function of emissivity can be performed by using the following set of equations [7]. A variation of the equilibrium temperature (ΔT) for a given variation of pressure (ΔP) is provided by the following equations:

$$\Delta \mathrm{T} = \left[\left(\Psi \cdot (\mathrm{T_o} - \mathrm{T_{eq}}) \cdot \frac{\Delta \mathrm{P}}{(\varepsilon \cdot \sigma)}\right) + {\mathrm{T_{eq}}}^4\right]^{1/4} - \mathrm{T_{eq}} \qquad (1)$$

where

$$\Psi = 1.5 \cdot \mathrm{k} \cdot \frac{\alpha}{(2\Pi \mathrm{m k T_o})^{1/2}}. \qquad (2)$$

In (1) and (2), $\mathrm{T_o}$ is the room temperature, $\mathrm{T_{eq}}$ is the equilibrium temperature, ΔP is the pressure variation, ε represents the emissivity of the material, σ is Stefan constant, k is Boltzman's constant, α determines the efficiency of energy transfer process, and m is the mass of air molecules. By considering $\mathrm{T_o} = 25\,^{\circ}\mathrm{C}$, $\mathrm{T_{eq}} = 175\,^{\circ}\mathrm{C}$, and $\alpha = 1$, the sensitivity variation as a function of decrease in emissivity has been evaluated for a pressure variation of 1 Pascal and the results are presented in Fig. 1.

Fig. 1 indicates that there is continuous improvement in the sensitivity of the device with decreasing emissivity of the substrate. After reaching a certain threshold lower value of emissivity, the sensitivity increases exponentially with a further decrease in the emissivity values.

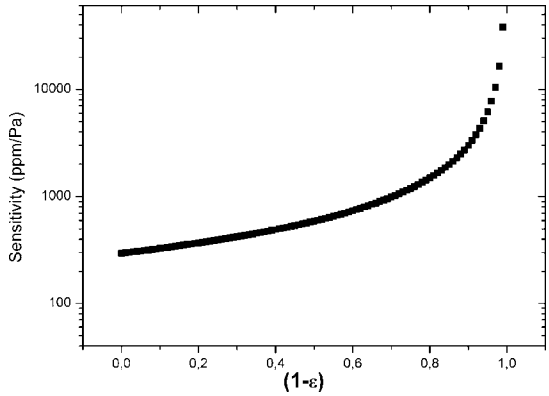

Fig. 1. Theoretical estimation of sensitivity as a function of decrease in emissivity values of the SAW device.

III. Sensor Structure

Fig. 2(a) represents a typical metallized structure of the device. Rayleigh SAW is generated and detected on the black $LiNbO_3$ substrate by using the IDTs. In order to check the effect of metallization, a thin layer ($\sim$150 nm) of aluminum was deposited on the backside of the substrate, and the corresponding device is abbreviated as a metallized device. Aluminum was chosen for its low value of emmissivity $\sim$0.04. The heater has been imprinted around the IDTs and near the corners of the substrate for uniform heating of the device. We have kept the gap between heater and IDT structures of the order of 100 μm for uniform heating of transmitting and receiving IDTs.

Cheap electronic components are easily available around 433 MHz because this frequency lies in the range of instruments, scientific, and metrology (ISM) category. Therefore, it is speculated that if more compatible electronic components are needed to upgrade the device (operating at 433 MHz) for its commercial utilization, then they can be procured from the commercial market conveniently. In order to fabricate SAW devices for the above mentioned frequency, design parameters have been estimated by using well-established coupling–of-modes (COM) theory [15]. The COM equations use a cascading relationship and the P-matrices for the IDTs which deal with acoustic waves propagating in the forward and reverse directions. Equations incorporate coupling interaction of SAWs. We have used software programs developed by K. Hashimoto [15]. In our case, we have used IDT period $=$ 9.2 μm, IDT width$=$ 50 μm, IDT aperture $=$ 1100 μm, number of IDT finger pairs $=$ 30, and the gap between transmitting and receiving IDT $=$ 375.2 μm. Fig. 2(b) shows the experimental S21 frequency response (amplitude and phase) of the SAW device. An insertion loss of better than $-$15 dB was observed in the S21 waveform. A very linear-phase waveform was observed around 433 MHz in a bandwidth of at least 3 MHz.

IV. Experiment

The planar black $LiNbO_3$ ($\mathrm{Y} + 128^{\circ} - \mathrm{X}$) substrate was employed during the investigations. Ti/Au IDTs with uniform spacing were deposited by the sputtering method. The heating resistor was directly printed on the SAW surface and was fabricated by lift-off technique. It was possible to inject desired

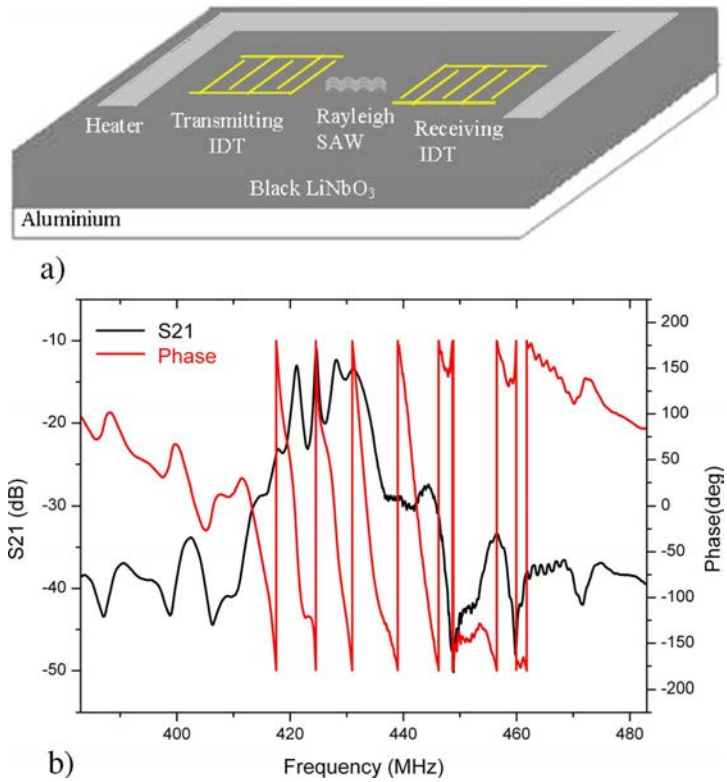

Fig. 2. (a) Metallized SAW device and (b) its associated experimental S21 and phase waveforms.

power into the device in order to control its temperature. When the power is injected into the SAW device, the temperature of the device increases. The power dissipation in the surrounding medium (by radiation and gas conduction) becomes the same as the power injected into the device and the temperature is stabilized which is called equilibrium temperature. The device was tested up to the maximum input power of 125 mW (equilibrium temperature $= 331\,^{\circ}$C for a nonmetallized device). The reported experimental frequency points at fixed phase were obtained with the help of the HP8752 network analyzer (Agilent Technologies, Santa Clara, CA). In order to thermally insulate the SAW device from the remaining experimental setup, it was suspended by wire bonding of 25 μm diameter. This technique has resulted in the improvement of the interaction between gas and SAW device. IDTs are connected to the printed-circuit board (PCB), RF equipment, and heater by wires. The RF signal is transmitted through the PCB, coaxial connector, and SMA to the characterization equipment. The heating power can also be transmitted through the same electrical DB9-type feed via the connector. Platinum has been used as material for heating resistor. Temperature at the device has been estimated from TCF and central frequency measurements of the device at different injected powers. A 2-D multiphysics finite-elements software (COMSOL) was used to design each part of the device by taking into account different materials and their properties, such as heat capacity, thermal conductivity, etc. [16]. Temperature was observed to be uniform along the acoustic-wave path. A detailed description of the SAW sensor and packaging has been presented elsewhere by the authors [8].

The TCF of the device was measured experimentally by heating the SAW device at regular intervals and measuring the frequency values at fixed phase and their corresponding temperatures. A negative value of the TCF was observed with the magnitude of 68 ppm/°C.

V. Results and Discussion

The SAW frequency carries the information about the pressure as well as the temperature variations. Room temperature variations lead to the background frequency variations which subsequently cause error in the measured frequency. Background frequency (f_b) due to room temperature variation has been calculated from TCF and central frequency data. It has been subtracted from the measured frequency (f_m), and the resulting frequency ($f_r = f_m - f_b$) is presented. Variation in room temperature has been measured by using platinum resistance in the vacuum chamber. Due to the incorporation of background frequency values in the resulting frequency values, it is not possible to measure the maximum resolution of the sensor which is limited by the sensitivity of platinum resistance. During future experiments, the authors plan to undertake experiments by using two SAW devices: one of them may act as a sensor and the other as reference. In this case, it would be possible to provide the true resolution of our device. During an experiment in the laboratory for almost 15 h at constant pressure ($2 \sim 3 \times 10^{-4}$ Pa) and for a room temperature variation of almost 6 centigrade, f_r was observed to have the standard deviation of ± 3 kHz which sets the limit of the accuracy of the results.

Fig. 3 justifies that the sensor works on the Pirani principle. It can be observed that the plot of frequency as a function of vacuum pressure is similar to the typical "S" shape characteristic curve of the Pirani gauge [6]. In the case of the conventional Pirani gauge, it is not possible to realize sensitivity above 10^2 Pa.

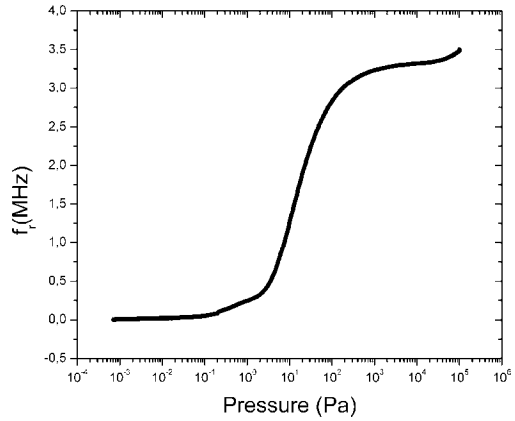

Fig. 3. Typical S-shape characteristic curve for the frequency (f_r) response as a function of vacuum pressure in the Pirani SAW device.

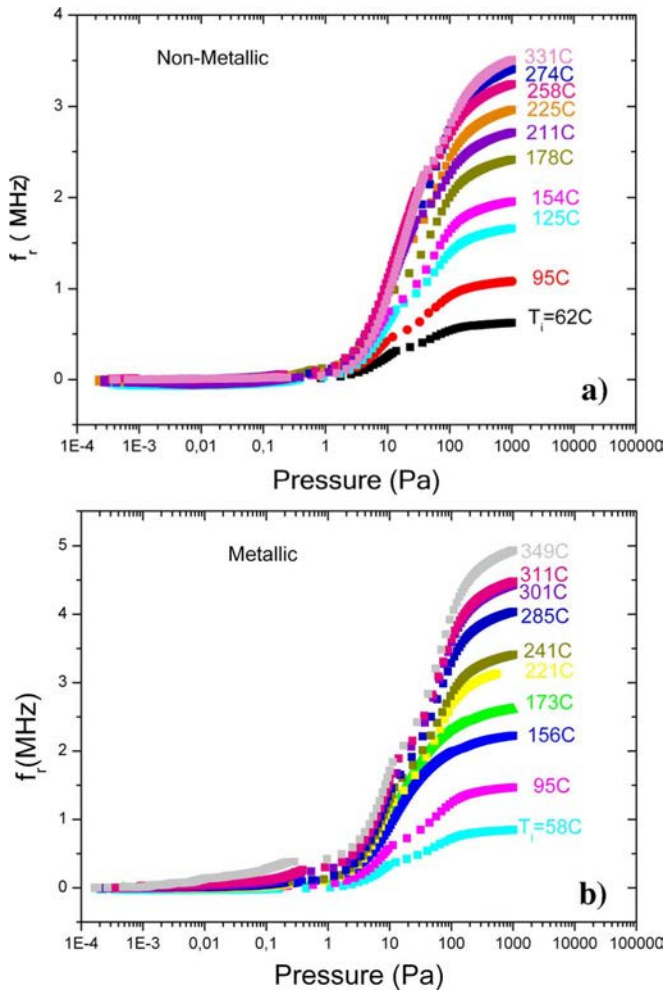

Fig. 4. Frequency (f_r) response as a function of vacuum pressure at different equilibrium temperatures for (a) nonmetallic and (b) metallic devices.

However, in our sensor, the development of a clear slope occurs above 10^4 Pa. This result clarifies that the Pirani SAW sensor has the advantage over the conventional Pirani gauge in terms of pressure sensitivity in a high-pressure region.

Frequency measurements are reported up to the maximum possible limit of the temperature for which the phase signal could be observed in nonmetallized and metallized SAW devices (Fig. 4). Measurements have been undertaken in a vacuum pressure range of 10^{-4} up to 10^3 Pa. Trends could be observed up to the initial equilibrium temperature of 349C (= 622 K) and 331C (= 604 K) for metallized and nonmetallized devices and after that, the phase signal was lost. In the case of normal $LiNbO_3$, it is possible to observe the phase signal up to 720 K. Bruckner *et al.* have carried out the acoustic attenuation loss measurements as a function of temperature for black and whiteLi niobate SAW ID tags [17]. They have found that attenuation of black compared to white $LiNbO_3$ rises quickly above 573 K. The maximum temperature for reporting attenuation data for a black $LiNbO_3$ is around 623 K which is very close to our maximum-achieved temperature before the disappearance of the phase signal (622 K). The similarity of the results proves the authenticity of our data. The black-and-white $LiNbO_3$ are expected to show an increase in bulk conductivity with the rise in temperature in the similar fashion as reported for langasite [18], [19]. In the light of this situation, it is speculated that with the rise in the temperature, the bulk conductivity of black as well as white $LiNbO_3$ increases to a point where electric fields are short-circuited and cannot drive the piezoelectric effect. Black as compared to white $LiNbO_3$ is expected to have higher electrical conductivity at room temperature. Therefore, it is speculated that during the increase in temperature, black $LiNbO_3$ acquires the sufficient electrical conductivity for failure at lower temperature (622 K) compared to white $LiNbO_3$ (720 K). The frequency change in metallized and nonmetallized SAW devices corresponds to 4.9 and 3.5 MHz, respectively (Fig. 4). The results indicate that aluminium thin-film deposition significantly improves the pressure sensitivity of the device.

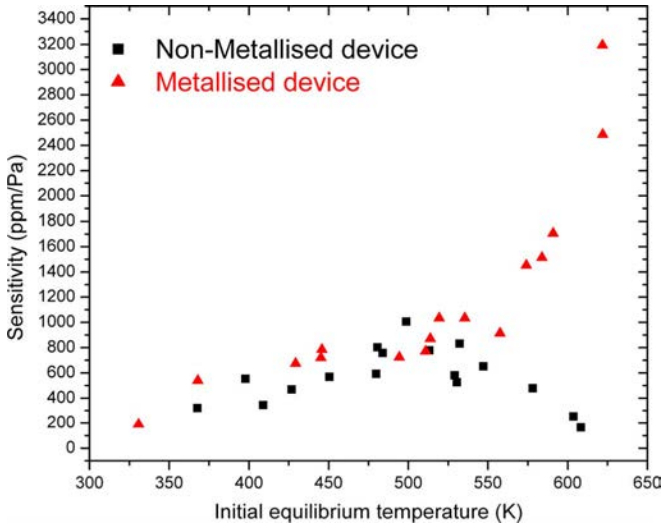

Fig. 5. Experimental sensitivities nonmetallized and metallized SAW devices as a function of initial equilibrium temperature.

Fig. 5 shows the trends of sensitivity variation as a function of initial equilibrium temperature for black $LiNbO_3$ piezoelectric material for the pressure variation in the region of 10^{-2} to 10^{-1} Pa. It can be seen that there is a remarkable similarity between the trends of experimental results of nonmetallized and metallized SAW devices up to 550 K. Above 550 K, sensitivity rises exponentially with the increase in initial equilibrium temperature for an aluminium-coated device in contrast to a non-

metallized device. The observed trends in Fig. 5 can be explained as follows. It is speculated that nonmetallized and metallized SAW devices have similar trends up to 550 K because aluminium and $LiNbO_3$ have almost a constant value of emissivity up to 550 K. Due to this reason, both follow the trends similar to experimental results as reported earlier for a conventional $LiNbO_3$-based SAW sensor [7]. Above 550 K, the emissivity of Al decreases with the rise in temperature in contrast to the constant value maintained by $LiNbO_3$. This conclusion has been drawn on the basis of the recently conducted emissivity measurements of commercial pure aluminium and aluminium alloys by Chang-Da Wen and Issam Mudawar in the temperature range of 600–800 K [20], [21]. It has been noticed that although there is a general trend of increase of emissivity with an increase in temperature for metallic surfaces, aluminium and most of the aluminium alloys buck this trend. For example, it has been observed that emissivity of pure aluminium (Al 1100) and aluminium alloys (Al 7075, Al 2024) decreases in the temperature range of 600 to 700 K [21]. A temperature of 600 K is very close to our value of temperature of 550 K for observing the exponential rise in sensitivity values. Trends of the theoretical estimated values of sensitivity as a function of decrease in emissivity, and experimental sensitivity as a function of increase in temperature of metallized device are very similar in qualitative terms (Figs. 1 and 5). Both show a continuous improvement in their sensitivity values and then for a threshold lower value of emissivity, there is suddenly an exponential improvement in the sensitivity values. In the light of the aforementioned observations, it is speculated that above 550 K, an exponential rise (in contrast to a decrease in sensitivity values of nonmetallized device) is related to the decrease in emissivity of aluminium with the rise in temperature. The relation between enhancement in sensitivity and the decrease in emissivity can be explained as follows. In the Knudsen regime, heat loss occurs with conduction and radiation phenomenon. The conduction is proportional to gas pressure. Therefore, in order to improve the sensitivity of the device, heat loss by radiation has to be minimized. In the event of injecting power into the SAW device, power dissipated in the surrounding medium by radiation (ΔP_e^{rad}) [7] is

$$\Delta P_e^{rad} = \varepsilon\sigma(T_f^4 - T_{eq}). \tag{3}$$

Here, T_f is the final equilibrium temperature. It is evident that a decrease of emissivity decreases the value of ΔP_e^{rad} and, hence, improves the sensitivity of the device. Furthermore, the quantitative estimation of sensitivity enhancement with the decrease in emissivity values can be realized from Fig. 1.

Threshold temperature value for observing the exponential increase in sensitivity values for metallized device has been observed as 550 K. It is speculated that in the event of the availability of phase signal above 622 K, it would have been possible to observe the exponential increase in the sensitivity values. In the light of these observations, authors predict that Al coating makes the sensitivity of SAW sensor temperature dependent. It might be possible to observe exponential rise in sensitivity values above 622 K by depositing aluminium thin film on suitable piezoelectric material having high TCF value, higher limit of operating temperature and low emissivity value. It is not possible to realize all the aforesaid parameters in a single piezoelectric material. Quartz ST-X seems to be optimum substrate. TCF value of this substrate is zero at room temperature (RT) and its magnitude increases with operating temperature [12]. This feature makes it possible to use quartz ST-X material to act as reference sensor due to its frequency stability at RT and also as highly sensitive Pirani-SAW sensor operating at high temperature. Quartz can be used for SAW applications up to 500C. Although, the phase transition from α to β phase in quartz occurs at 573C but the material fails around 500C due to twin formation [12]. The mechanical stress of SAW enhancement and temperature leads to the formation of twinning defects. In our case, we need the substrate with a high value of TCF at high temperature. Although ST-X quartz has an almost zero value of TCF at room temperature, it increases with the rise in temperature. For example, the TCF value for ST-X quartz at 200, 300, and 400C are -20, -30, and -40 ppm/C, respectively [12]. In the light of this situation, ST-X quartz meets our requirements for future experiments at higher temperatures. The future vacuum sensor may be fabricated by the deposition of Al thin film on quartz, and it is speculated that it will be possible with the new device to enhance the lower limit of vacuum pressure measurement up to 10^{-5} Pa.

The vacuum chamber housing the Pirani gauge and SAW device has been rapidly pumped from almost 10^3 to 10^{-2} Pa. The time to achieve a 63% decrease in the amplitude of the transition region has been evaluated and reported as the response time. Measured response times of Pirani and SAW devices are 7 and 40 s, respectively. Although the Pirani SAW device provides the promising solution as a sensor for wide pressure-range measurements, its current drawback is the response time which is relatively high. It might be possible to improve the response time by decreasing the time required by the device to reach thermal equilibrium. In order to achieve this target, one possible way is to increase the ratio of surface area to the volume of the device. This can be achieved with the construction of the device on a thin planar substrate. The thinner device has larger resistivity in the bulk and, hence, it needs lower power to achieve the desired temperature at the substrate. Although, very thin substrates have small volume but they are extremely fragile. Therefore, in the case of the thin planar substrate-based device, a compromise has to be made between response time, fragility, and power consumption properties of the device. In the light of this situation, in future experiments, we will estimate the optimum thickness of the substrate by measuring the response times, sound velocities, and power injected into the substrates with different thicknesses.

Maximum sensitivity observed for the metallized device is 1.38 MHz/Pa which is three times higher compared to maximum sensitivity (0.44 MHz/Pa) observed for the nonmetallized SAW device. Correspondingly, the frequency response obtained as a function of vacuum pressure is plotted in Fig. 6. The sdvantage of a metallized device in terms of higher slope is explicitly visible at higher pressure. In order to show the improvement in the lower vacuum pressure region, we have plotted the frequency response in low vacuum pressure in the inset. Initial frequency values for metallized and nonmetallized devices have been shifted to zero for making a useful comparison. It can be

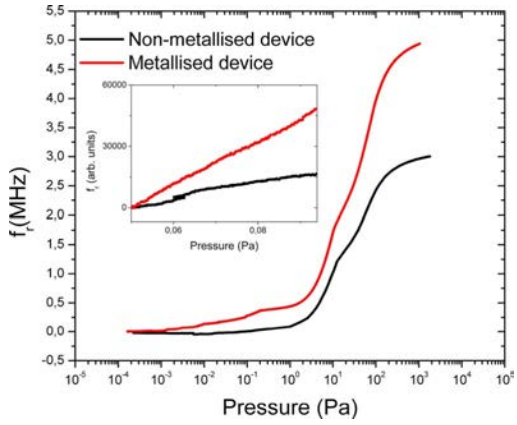

Fig. 6. Frequency (f_r) response as a function of vacuum pressure corresponding to maximum sensitive values observed for nonmetallized and metallized devices.

seen that the metallized sensor has a better slope in the low-pressure regime. These observations demonstrate that the metallized device has better accuracy for vacuum pressure measurements for low as well as high vacuum pressure regions.

VI. Conclusion

The deposition of thin film of the aluminum on black $LiNbO_3$ substrate improves the pressure sensitivity of the SAW device with the rise in temperature. After achieving a critical temperature, sensitivity increases exponentially with a further increase in temperature in contrast to a nonmetallized device which shows a decrease in the sensitivity values. The obtained results can contribute to the development of a miniature pressure sensor based on SAW technology which can be used under harsh environments, such as high temperature.

References

[1] S. Chatterjee, A. K. Halder, K. Sengupta, and H. S. Maiti, "A vacuum gauge using positive temperature coefficient thermistor as the sensor," *Rev. Sci. Instrum.*, vol. 71, pp. 4670–4673, 2000.

[2] F. Volklein and A. Meier, "Microstructured vacuum gauges and their future perspectives," *Vacuum*, vol. 82, pp. 420–430, 2007.

[3] R. Puers, S. Reyntjens, and D. De Bruyker, "The NanoPirani – An extremely miniaturized pressure sensor fabricated by focused ion beam rapid prototyping," *Sens. Actuators, A*, vol. 97–98, pp. 208–214, 2002.

[4] M. Doms, A. Bekesch, and J. Mueller, "A microfabricated Pirani pressure sensor operating near atmospheric pressure," *J. Micromech. Microeng.*, vol. 15, pp. 1504–1510, 2005.

[5] G. Bedo, W. Kraus, and R. Muller, "Comparison of different micromechanical vacuum sensors," *Sens. Actuators*, vol. A 85, pp. 181–188, 2000.

[6] K. Khosraviani and A. M. Leung, "The nanogap Pirani – A pressure sensor with superior linearity in an atmospheric pressure range," *J. Micromech. Microeng.*, vol. 19, no. Art. no. 045007, pp. 2009–2009.

[7] P. Nicolay, O. Elmazria, F. Sarry, L. Bouvot, N. Marche, and H. Kambara, "Innovative surface acoustic wave sensor for accurate measurement of subatmospheric pressure," *Appl. Phys. Lett.*, vol. 92, no. Art. no. 141909, 2008.

[8] P. Nicolay, O. Elmazria, F. Sarry, L. Bouvot, H. Kambara, K. J. Singh, and P. Alnot, "Wide vacuum pressure range monitoring by Pirani SAW sensor," *IEEE Trans. Ultrason. Ferroelectron. Frequency Control*, vol. 57, no. 3, pp. 684–689, Mar. 2010.

[9] D. Morgan, *Surface Acoustic Wave Filters*, 2nd ed. New York: Elsevier, 2007.

[10] S. I. Shikata, *Low-Pressure Synthetic Diamond*, B. Dischler and C. Wild, Eds. New York: Springer, 1998, Springer Series in Materials, Processing, p. 261.

[11] C. K. Campbell, *Surface Acoustic Wave Devices for Mobile and Wireless Communications*. New York: Academic, 1998.

[12] J. Hornsteiner, E. Born, G. Fischerauer, and E. Riha, "Surface acoustic wave sensors for high temperature applications," in *Proc. IEEE Int. Frequency Control Symp.*, 1998, pp. 615–620.

[13] P. F. Bordui, D. H. Jundt, E. M. Standifer, R. G. Norwood, R. L. Sawin, and J. D. Galipeau, "Chemically reduced lithium niobate single crystals: Processing, properties and improved surface acoustic wave device fabrication and performance," *J. Appl. Phys.*, vol. 85, pp. 3766–3769, 1999.

[14] S. Jen and R. Bobkowski, "Black lithium niobate SAW device fabrication and performance evaluation," in *Proc. IEEE Ultrasonics Symp.*, 2000, pp. 269–273.

[15] K. Y. Hashimoto, *Surface Acoustic Wave Devices in Telecommunications*. New York: Springer, 2000.

[16] P. Nicolay, O. Elmazria, F. Sarry, T. Aubert, L. Bouvot, and M. Hehn, "New measurement method to characterize piezoelectric SAW substrates at very high temperature," in *Proc. IEEE Int. Ultrasonics Symp.*, 2008, pp. 1877–1880.

[17] G. Bruckner, R. Hauser, A. Stelzer, L. Maurer, L. Reindl, R. Teichmann, and J. Biniasch, "High temperature stable SAW based tagging system for identifying a pressure sensor," in *Proc. IEEE Int. Frequency Control Symp. PDA Exhibit.*, 2003, pp. 942–47.

[18] H. Fritze, M. Schulz, H. Seh, and H. L. Tuller, "High temperature operation and stability of langasite resonators," in *Proc. Mat. Res. Soc. Symp.*, 2005, vol. 828, pp. A3.9.1/K4.9.1–A3.9.6/K4.9.6.

[19] T. Taishi, T. Hayashi, N. Bamba, Y. Ohno, I. Yonenaga, and K. Hoshikawa, "Oxygen defects in langasite ($La_3Ga_5SiO_{14}$) single crystal grown by vertical Bridgman (VB) method," *Phys. B*, vol. 401–402, pp. 437–440, 2007.

[20] C. D. Wen and I. Mudawar, "Emissivity characteristics of polished aluminium alloy surfaces and assessment of multispectral radiation thermometry (MRT) emissivity models," *Int. J. Heat Mass Transfer*, vol. 48, pp. 1316–1329, 2005.

[21] C. D. Wen and I. Mudawar, "Modelling the effects of surface roughness on the emissivity of aluminium alloy," *Int. J. Heat Mass Transfer*, vol. 49, pp. 4279–4289, 2006.